Multiantenna-Assisted Spectrum Sensing for Cognitive Radio

Pu Wang, *Student Member, IEEE*, Jun Fang, *Member, IEEE*, Ning Han, *Student Member, IEEE*, and Hongbin Li, *Senior Member, IEEE*

***Abstract*—In this paper, we consider the problem of detecting a primary user in a cognitive radio network by employing multiple antennas at the cognitive receiver. In vehicular applications, cognitive radios typically transit regions with differing densities of primary users. Therefore, speed of detection is key, and so, detection based on a small number of samples is particularly advantageous for vehicular applications. Assuming no prior knowledge of the primary user's signaling scheme, the channels between the primary user and the cognitive user, and the variance of the noise seen at the cognitive user, a generalized likelihood ratio test (GLRT) is developed to detect the presence/absence of the primary user. Asymptotic performance analysis for the proposed GLRT is also presented. A performance comparison between the proposed GLRT and other existing methods, such as the energy detector (ED) and several eigenvalue-based methods under the condition of unknown or inaccurately known noise variance, is provided. Our results show that the proposed GLRT exhibits better performance than other existing techniques, particularly when the number of samples is small, which is particularly critical in vehicular applications.**

***Index Terms*—Cognitive radio (CR), generalized likelihood ratio test (GLRT), spectrum sensing.**

I. Introduction

RECENTLY, there has been a dramatic increase in the demand for a radio spectrum, primarily due to the evolution of various wireless networks driven by the increasing needs of consumers in wireless services. The inflexibility of traditional spectrum-management approaches also causes the scarcity of the radio spectrum. The frequency bands are exclusively licensed to systems, and their users have to operate within an allocated frequency band. However, only a small portion of the spectrum is used in the U.S. at any given time/location: The current utilization of a licensed spectrum varies from 15% to 85% [1].

Motivated by the demand for the radio spectrum, the concept of opportunistic spectrum access has attracted significant attention over the past few years. Opportunistic spectrum access allows secondary users share the spectrum with licensed users (also called primary users) without causing harmful interference. Cognitive radio (CR), which was first proposed by Mitola [2], [3], is considered to be a promising technology for implementing opportunistic spectrum access. A CR system is an intelligent wireless communication system that is aware of its surrounding environment, learns from the environment, and adapts its operating parameters in real time [4]. One fundamental requirement of this system is the ability to identify the white space in the spectrum of interest by the secondary users. Therefore, spectrum sensing should be periodically performed to efficiently recognize the operation of primary user systems and other CR systems [5]–[7].

Generally, spectrum-sensing methods include matched filter detection [8]–[11], energy detection [12]–[15], and cyclostationary feature detection [16]–[18]. Each of them has its advantages and disadvantages. Cyclostationary detection needs to know the cyclic frequencies of the primary signal, which may not be available to the secondary users in practice. Also, it has high computational complexity. Matched filter-based detection is considered to be an optimal signal-detection method. However, it requires *a priori* knowledge of the primary user, e.g., modulation type, pulse shaping, and synchronization of timing and carrier. Moreover, for the matched filter detection, the CR will need a dedicated receiver for every primary user, which makes it difficult for practical implementation [19]. As compared with the above two categories of approaches, energy detection requires no information of the primary signal and is robust to the unknown channels. This makes it a very desirable spectrum-sensing technique for the CR.

The problem with the energy detector (ED), however, is that it requires the knowledge of the noise variance to correctly set the test threshold to meet a selected false-alarm probability. In practice, the noise variance has to be estimated by some estimation procedure, which is subject to various errors that are introduced by the detection device and environment, e.g., temperature, humidity, device aging, radio interference, etc. It has been found that the ED is fairly sensitive to the accuracy of the estimated noise variance [20]. To circumvent this difficulty, without estimating the noise variance, [21] proposed a method that involves a multiantenna receiver. The method is referred to as the maximum-to-minimum ratio eigenvalue (MME) detector, which employs the ratio of the maximum eigenvalue to the minimum eigenvalue of the covariance matrix of the received signal. The performance is evaluated by resorting to the random matrix theory, and the threshold for detection is given in a

Manuscript received May 21, 2009; revised September 20, 2009. First published December 4, 2009; current version published May 14, 2010. This work was supported in part by the National Science Foundation under Grant CCF-0514938 and Grant ECCS-0901066 and in part by the Air Force Office of Scientific Research under Grant FA9550-09-1-0310. The review of this paper was coordinated by Dr. W. Zhuang.

The authors are with the Department of Electrical and Computer Engineering, Stevens Institute of Technology, Hoboken, NJ 07030 USA (e-mail: pwang4@stevens.edu; Jun.Fang@stevens.edu; nhan@stevens.edu; Hongbin.Li@stevens.edu).

Color versions of one or more of the figures in this paper are available online at http://ieeexplore.ieee.org.

Digital Object Identifier 10.1109/TVT.2009.2037912

closed form. By treating the noise variance or the covariance matrix of the received signal as unknown, [22] developed a new detector under the generalized likelihood ratio test (GLRT) framework. The test statistic is the arithmetic-to-geometric mean (AGM) of the eigenvalues of the estimated covariance matrix, and hence, the detector is referred to as the AGM detector. The authors also showed that, under the condition that the signal subspace is rank 1, the AGM detector reduces to the previous MME detector. Even though it is effective, these works [21], [22] did not fully exploit the signal structure that is inherent in the received signal. This, to some extent, degrades their detection performance.

In this paper, we consider the scenario where multiple receiver antennas are used, and there is only one primary signal to be detected. In this case, the signal covariance matrix can be modeled as a rank 1 matrix that is an outer product of the channel vector and its Hermitian (assuming that the primary user has only one transmitter). By exploiting this inherent signal structure, we develop a new GLRT detector. The proposed detector requires no prior knowledge of the transmitted signal, the wireless channel from the primary transmitter to the CR receiver, and the noise variance. The test statistic of the proposed detector admits a simple form that is given by the ratio of the largest eigenvalue to the sum of eigenvalues of the sample covariance matrix of the received signal. By fully exploiting the signal structure, our detector is able to achieve better performance than other existing methods when the noise variance is unknown. Numerical results are provided to show the effectiveness of our proposed detector.

The rest of this paper is organized as follows. In Section II, the signal model and prior solutions are briefly reviewed. Our GLRT-based spectrum sensing is presented in Section III, along with the underlying maximum-likelihood (ML) estimator for the unknown parameters and the asymptotic performance analysis. Performance of the multichannel ED is provided in Section IV. Numerical results are provided to evaluate the performance of our GLRT-based spectrum-sensing technique in Section V. Conclusions are drawn in Section VI. Mathematical derivations are mostly contained in Appendixes I–IV.

II. Signal Model and Prior Solutions

As in [21] and [22], we consider the scenario where multiple antennas are employed by the secondary user to detect the primary signal. The spectrum sensing problem can be formulated as the following binary hypothesis test:

$$\begin{aligned} H_0: &\quad \mathbf{x}(n) = \mathbf{w}(n), &\quad n = 0, \ldots, N-1 \\ H_1: &\quad \mathbf{x}(n) = \mathbf{s}(n) + \mathbf{w}(n), &\quad n = 0, \ldots, N-1 \end{aligned} \tag{1}$$

where $\mathbf{x}(n)$ denotes the $M \times 1$ baseband equivalent of the nth sample of the received signal, $\mathbf{s}(n)$ is the nth sample of the primary signal seen at the multiantenna receiver, and $\mathbf{w}(n)$ is assumed complex Gaussian noise that is independent of $\mathbf{s}(n)$ with unknown noise variance σ_w^2, i.e., $\mathbf{w}(n) \sim \mathcal{CN}(0, \sigma_w^2 \mathbf{I}_M)$. The multichannel signal $\mathbf{s}(n)$ can be expressed as $\mathbf{s}(n) = \mathbf{h}d(n)$, where a frequency nonselective fading channel is assumed, $\mathbf{h}$ denotes the $M \times 1$ channel coefficient, and $d(n)$ denotes the symbols that are transmitted by the primary user. Since the primary users' symbols are unknown, it is customary to assume that $\mathbf{s}$ is circularly symmetric Gaussian-distributed with zero mean and covariance matrix $\mathbf{R}_s = \mathbf{h}\mathbf{h}^H$ [assuming, without loss of generality, that $d(n)$ has unit energy] [22]. The assumption is typically used only for the derivation (not testing) of spectral sensing algorithms.

A. ED

The ED is a popular choice for spectrum sensing for CR applications. Urkowitz's [12] classical single-channel ED can easily be extended to the multichannel case, which takes the following form:

$$T_{\mathrm{ED}} = \sum_{n=0}^{N-1} \|\mathbf{x}(n)\|^2 \underset{H_0}{\overset{H_1}{\gtrless}} \gamma_{\mathrm{ED}} \tag{2}$$

where $\|\cdot\|$ denotes the standard vector norm, and the threshold γ_{ED} can be determined from a given probability of false alarm. Since the distribution of T_{ED} under H_0 depends on the noise variance σ_w^2, the threshold should be selected with the knowledge of σ_w^2.

However, in practice, the noise variance is usually unknown. As a result, the ED has to select the threshold by replacing the noise variance by its estimate. Let the estimated noise variance be $\hat{\sigma}_w^2 = \eta\sigma_w^2$, where η reflects on how accurate the estimate is. The noise uncertainty factor can be defined as $B = 10\log_{10}\eta$ in a deterministic way. The use of the constant factor B is based on the assumption that the noise is stationary and ergodic, which is usually valid when the observation time that is used for energy detection is short. Therefore, the ED with B-dB noise uncertainty is

$$T_{\text{ED-U}} = \sum_{n=0}^{N-1} \|\mathbf{x}(n)\|^2 \underset{H_0}{\overset{H_1}{\gtrless}} \gamma_{\text{ED-U}} \tag{3}$$

where the notation "ED-U" stands for the ED with uncertainty in noise power, and $\gamma_{\text{ED-U}}$ is determined by using the estimated noise variance to meet a given probability of false alarm. In the single-channel case, it has been shown in several studies [20]–[22] that the performance of the single-channel ED significantly degrades, even with a small amount of noise uncertainty. An examination of the performance of the multichannel EDs of (2) and (3) is included in Section IV, and the results also show that the multichannel ED is sensitive to the noise uncertainty.

B. AGM Detector

The above ED is equivalent to the estimator–correlator under the condition that the primary signals are white Gaussian [22], [23]. In [22], the primary user signal is modeled as colored Gaussian with unknown covariance matrix $\mathbf{R}_s$. A GLRT procedure is applied to the problem, which finds an unstructured estimate of $\mathbf{R}_x$, which is equivalent to $\mathbf{R}_s + \sigma_w^2\mathbf{I}$ under H_1 and σ^2 under H_0. The resulting detector computes the AGM of the eigenvalues of a sample covariance matrix and compares it with a threshold

$$T_{\mathrm{AGM}} = \frac{\frac{1}{M}\sum_{m=1}^{M}\hat{\lambda}_m}{\left(\prod_{m=1}^{M}\hat{\lambda}_m\right)^{1/M}} \underset{H_0}{\overset{H_1}{\gtrless}} \gamma_{\mathrm{AGM}} \tag{4}$$

where γ_{AGM} is a threshold determined from a given probability of false alarm, and λ_m is the mth largest eigenvalue of the following sample covariance matrix:

$$\hat{\mathbf{R}}_x = \frac{1}{N}\mathbf{X}\mathbf{X}^H \tag{5}$$

where $\mathbf{X} = [\mathbf{x}(0), \mathbf{x}(1), \ldots, \mathbf{x}(N-1)]$. Compared with the multichannel ED with inaccurate knowledge of the noise variance, the AGM detector is found to obtain improved spectrum-sensing performance when the noise variance is unknown.

C. MME Detector

For the case when the signal subspace is rank 1, [22] presents a two-step approach: First, it develops a GLRT scheme by assuming that the noise variance is known, and then, it replaces the noise variance of the GLRT by the smallest eigenvalue $\hat{\gamma}_M$ of the sample covariance matrix. The resulting detector computes the ratio of the maximum to the minimum ratio eigenvalues of the sample covariance matrix and is compared with a threshold

$$T_{\mathrm{MME}} = \frac{\hat{\lambda}_1}{\hat{\lambda}_M} \underset{H_0}{\overset{H_1}{\gtrless}} \gamma_{\mathrm{MME}} \tag{6}$$

where γ_{MME} is a threshold for a probability of false alarm. Without knowledge of the noise variance, the MME detector is shown to outperform the multichannel ED with noise uncertainty. This approach, however, does not fully exploit the inherent signal structure, i.e., the rank 1 property of the signal covariance matrix, and, consequently, degrades its detection performance.

III. Generalized Likelihood Ratio Test for Spectrum Sensing

Here, a GLRT is developed by exploiting the inherent signal structure and treating the noise variance as an unknown parameter. ML parameter estimation underlying the GLRT scheme is also examined. The general form of the GLRT for the problem of interest can be written as

$$T_{\mathrm{GLR}} = \frac{\max_{\mathbf{h},\sigma_w^2} p\left(\mathbf{X} \mid H_1, \mathbf{h}, \sigma_w^2\right)}{\max_{\sigma_w^2} p\left(\mathbf{X} \mid H_0, \sigma_w^2\right)} \tag{7}$$

where $p(\mathbf{X} \mid H_1, \mathbf{h}, \sigma_w^2)$ and $p(\mathbf{X} \mid H_0, \sigma_w^2)$ denote the likelihood functions under H_1 and H_0, respectively, i.e.,

$$p\left(\mathbf{X} \mid H_0, \sigma_w^2\right) = \prod_{n=0}^{N-1} \frac{1}{\pi^M \sigma_w^{2M}} \exp\left[-\frac{\mathbf{x}^H(n)\mathbf{x}(n)}{\sigma_w^2}\right] \tag{8}$$

$$\begin{aligned} p\left(\mathbf{X} \mid H_1, \mathbf{h}, \sigma_w^2\right) = &\prod_{n=0}^{N-1} \frac{1}{\pi^M \left|\mathbf{h}\mathbf{h}^H + \sigma_w^2\mathbf{I}\right|} \\ &\times \exp\left[-\mathbf{x}^H(n)\left(\mathbf{h}\mathbf{h}^H + \sigma_w^2\mathbf{I}\right)^{-1}\mathbf{x}(n)\right]. \end{aligned} \tag{9}$$

A. ML Estimation Under H_1 and H_0

The GLRT requires the ML estimates of unknown parameters under both hypotheses. To this end, the ML estimates of unknown parameters are developed and summarized in the following proposition.

Proposition: Given the signal model in (1), the ML estimates of unknown parameters $\mathbf{h}$ and σ_w^2 under H_1 and σ_w^2 under H_0 are given as

$$\hat{\mathbf{h}}_{\mathrm{ML}} = \left(\hat{\lambda}_1 - \frac{1}{M-1}\sum_{m=2}^{M}\hat{\lambda}_m\right)^{1/2} \mathbf{U}_x[:,1] \tag{10}$$

$$\hat{\sigma}_{w,H_1}^2 = \frac{1}{M-1}\sum_{m=2}^{M}\hat{\lambda}_m \tag{11}$$

$$\hat{\sigma}_{w,H_0}^2 = \frac{1}{M}\sum_{m=1}^{M}\hat{\lambda}_m \tag{12}$$

where $\hat{\mathbf{h}}_{\mathrm{ML}}$ is the ML estimate of $\mathbf{h}$ with an unknown ambiguous phase term, i.e., $\mathbf{h}\exp\{j\phi\}$, $\mathbf{U}_x$ is obtained by carrying out the eigenvalue decomposition (EVD) of the sample covariance matrix, i.e., $\hat{\mathbf{R}}_x = \mathbf{U}_x\mathbf{D}_x\mathbf{U}_x^H$, and the diagonal elements of $\mathbf{D}_x = \mathrm{diag}[\hat{\lambda}_1, \ldots, \hat{\lambda}_M]$ are in a descending order.

Proof: See Appendix I. ■

It is shown that the vector $\hat{\mathbf{h}}_{\mathrm{ML}}$ is the product between the eigenvector associated with the largest eigenvalue and the difference between the largest eigenvalue and the mean of the remaining $M-1$ eigenvalues; the ambiguous phase term in $\hat{\mathbf{h}}_{\mathrm{ML}}$ is standard in blind estimation (the cognitive receiver has no prior knowledge of the transmitted signal of the primary user), although it has no impact on our GLRT, which is a noncoherent detector; the ML estimate of the noise variance under H_1 is the mean of the smallest $M-1$ eigenvalues of the sample covariance matrix; and the ML estimate of the noise variance under H_0 is the mean of the M eigenvalues of the sample covariance matrix.

B. GLRT Test Statistic

With the ML estimates of unknown parameters under both hypotheses, the GLRT can be obtained as

$$T_{\mathrm{GLR}} = \frac{\hat{\lambda}_1}{\sum_{m=1}^{M}\hat{\lambda}_m} \underset{H_0}{\overset{H_1}{\gtrless}} \gamma_{\mathrm{GLR}} \tag{13}$$

where γ_{GLR} is a threshold determined from a given probability of false alarm. The derivation of the GLRT statistic is detailed in Appendix II. From (13), it is shown that the final GLRT statistic is a ratio of the largest eigenvalue to the sum of eigenvalues of the sample covariance matrix. It is shown that the proposed GLRT requires no *a priori* knowledge of the noise variance and, therefore, is more robust to the noise uncertainty than the multichannel ED. Compared with the AGM detector (6), the proposed GLRT estimates the noise variance by using eigenvalues that are associated with the noise subspace and, hence, is more robust.

The underlying assumption of the signal model in Section II is that the channel vector remains fixed over the observation interval. In real applications, the channel may experience some time-varying fading. The proposed detector can be adaptively implemented to provide some resistance, as long as the channel variation over the observation window (of N samples) is small. The idea is to compute a time-varying covariance matrix as follows:

$$\hat{\mathbf{R}}_x(t)=\hat{\mathbf{R}}_x(t-1)+N^{-1}\left[\mathbf{x}(t)\mathbf{x}^H(t)-\mathbf{x}(t-N)\mathbf{x}^H(t-N)\right]. \tag{14}$$

In essence, the above equation forms a time-varying covariance matrix estimate by using a sliding window of duration N samples. Each time a new observation $\mathbf{x}(t)$ becomes available, it is used to replace the oldest observation $\mathbf{x}(t-N)$ in updating the covariance matrix and the corresponding eigenvalues. This allows the GLRT detector to be updated on a sample-by-sample basis. Such an adaptive implementation, which provides some tracking capability to a slowly time-varying fading channel, has been widely used for time-varying channel estimation (see, e.g., [24] for additional details and numerical results).

C. Asymptotic Performance of the GLRT

As shown in Appendix III, i.e., the asymptotic performance of the GLRT, the asymptotic distribution of the log-GLRT statistic in (39) is given by

$$T_{\log\text{-GLR}} \overset{a}{\sim} \begin{cases} \chi^2_{2M-1}, & \text{under } H_0 \\ \chi'^2_{2M-1}(\lambda), & \text{under } H_1 \end{cases} \tag{15}$$

where χ^2_{2M-1} denotes the central chi-square distribution with $2M-1$ degrees of freedom and $\chi'^2_{2M-1}(\lambda)$ the noncentral chi-square distribution with $2M-1$ degrees of freedom and noncentrality parameter λ given by

$$\lambda = \frac{N(M-1)(\mathbf{h}^H\mathbf{h})^2}{M\sigma_w^4}. \tag{16}$$

Using the above result, we can write the asymptotic detection and false-alarm probabilities as

$$P_d = Q_{M-0.5}(\sqrt{\lambda}, \sqrt{\gamma_{\mathrm{GLR}}}) \tag{17}$$

$$P_f = \frac{\bar{\Gamma}(M-0.5, \gamma_{\mathrm{GLR}})}{\Gamma(M-0.5)} \tag{18}$$

where $Q_m(a,b)$ is the generalized Marcum-Q function, $\bar{\Gamma}(\cdot,\cdot)$ is the lower incomplete Gamma function, and $\Gamma(\cdot)$ denotes the Gamma function [25].

IV. Performance of Multichannel Energy Detection

For comparison purposes, the performance of the multichannel EDs, i.e., (2) and (3), is examined by calculating both probabilities of detection and false alarm. Appendix IV includes the details of the derivation, and the results are summarized below.

Multichannel ED Without Noise Uncertainty [See (2)]: By assuming perfect knowledge of the noise variance, probabilities of detection and false alarm for the multichannel ED (2) are expressed in closed forms as

$$P_f = \frac{\bar{\Gamma}\left(MN, \gamma/\sigma_w^2\right)}{\Gamma(MN)} \tag{19}$$

$$P_d = Q_{MN}\left(\sqrt{2\rho}, \sqrt{\frac{2\gamma}{\sigma_w^2}}\right). \tag{20}$$

Multichannel ED With Noise Uncertainty [See (3)]: Under the condition that the noise variance is unknown, probabilities of detection and false alarm for the multichannel ED with noise uncertainty (3) are shown as

$$P_f = \frac{\bar{\Gamma}\left(MN, \gamma/\left(\eta\sigma_w^2\right)\right)}{\Gamma(MN)} \tag{21}$$

$$P_d = Q_{MN}\left(\sqrt{2\rho}, \sqrt{\frac{2\gamma}{\sigma_w^2}}\right). \tag{22}$$

With the above probabilities of detection and false alarm, we can examine the sensitivity of the multichannel ED to the noise uncertainty, i.e., η (equivalently, the noise uncertainty factor B in decibels), via the receiver operating characteristic (ROC). Fig. 1 shows the ROC curves of the multichannel EDs with a number of noise uncertainties. When $P_f = 0.01$, SNR $=-1$ dB, $M = 4$, and $N = 4$, it is shown that the performance loss is about 0.2 and 0.4 in P_d with 0.5- and 1-dB noise uncertainties, respectively, with respect to that of the multichannel ED with accurate noise variance.

V. Numerical Examples

Here, we present simulation results to illustrate the performance of the proposed detection techniques and compare them with other existing techniques. Throughout this section, we assume that the secondary receiver has $M = 4$ antennas, whereas the transmitter has only one transmit antenna sending independent binary phase shift keying signals. In this case, the covariance matrix for the receiving signal is rank 1. Moreover, independent Rayleigh fading channels are simulated between

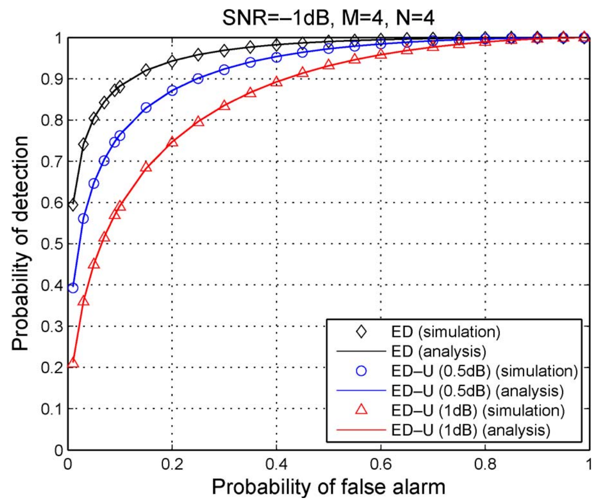

Fig. 1. ROC curves for multichannel energy detectors (2) and (3) when $M = 4$, $N = 4$, and $\mathrm{SNR} = -1$ dB.

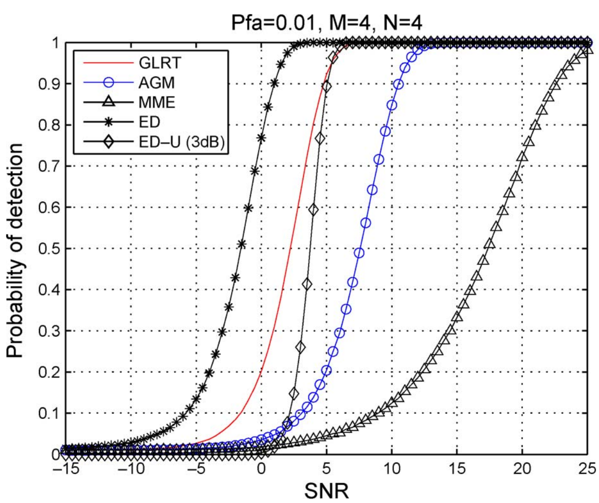

Fig. 2. Probability of detection versus SNR when $P_{\mathrm{fa}} = 0.01$, $M = 4$, and $N = 4$.

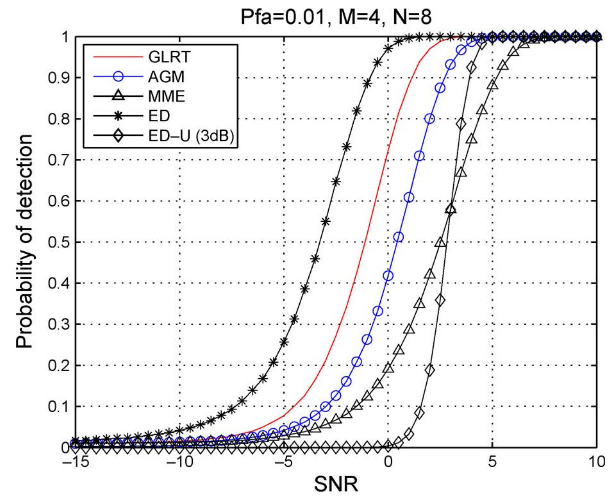

Fig. 3. Probability of detection versus SNR when $P_{\mathrm{fa}} = 0.01$, $M = 4$, and $N = 8$.

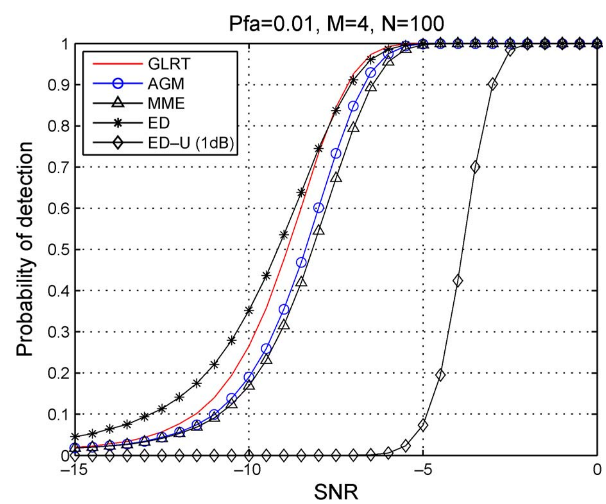

Fig. 4. Probability of detection versus SNR when $P_{\mathrm{fa}} = 0.01$, $M = 4$, and $N = 100$.

transmit–receiver antenna pairs. The probability of false alarm is fixed to 0.01.

Various cases of N (the number of samples) are considered from Figs. 2–4. In each case, the ED [see (2)], the ED-U [see (3); denoted as the ED-U (x dB), where the noise uncertainty factor x is shown in the figures], the AGM detector, and the MME detector are simulated for performance comparison with respect to the proposed GLRT. Note that the ED assumes perfect knowledge of the noise variance and, therefore, cannot be used in practice but offers a baseline for comparison. Moreover, we would use a large noise uncertainty factor $B = 3$ dB when the number of samples is small, e.g., $N = 4$ and $N = 8$, while choosing $B = 1$ dB and $B = 0.5$ dB when N is large.

From Figs. 2–4, a number of observations are made as follows.

- The proposed GLRT provides better performance than the ED-U, the AGM detector, and the MME detector for all cases of N. When N is small, our GLRT provides much better performance than the AGM detector and the MME detector. For example, when $N = 4$ and the probability of detection is 0.6, the performance gain of the GLRT is about 5 dB and more than 15 dB for the AGM and MME detectors.
- When the number of samples is small, the performance of the GLRT is generally worse than that of the ED. The performance gap is about 4 dB at $N = 4$ and about 2 dB at $N = 8$. When N is large, our results show that our GLRT can provide better performance than the ED at a high SNR.
- More samples are helpful to improve the detection performance for all detectors. This is due to the more accurate estimate of the covariance matrix with more samples. When $N = 100$, the GLRT, the ED, the AGM detector, and the MME detector all perform well. Specifically, our GLRT provides a marginal performance gain of about 0.5 and 0.7 dB over the AGM and the MME, respectively, when the probability of detection is 0.6.

Fig. 5 compares the detection performance of the GLRT for various values of N. It is seen again that the performance of the GLRT benefits from more samples. It is noted that the amounts

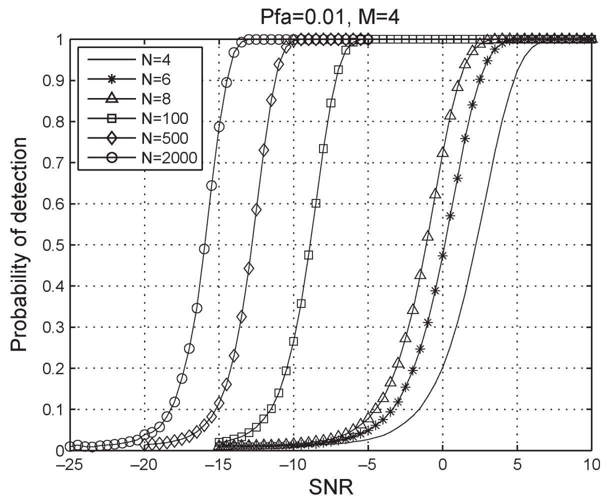

Fig. 5. Probability of detection versus SNR for different values of N when $P_{\text{fa}} = 0.01$ and $M = 4$.

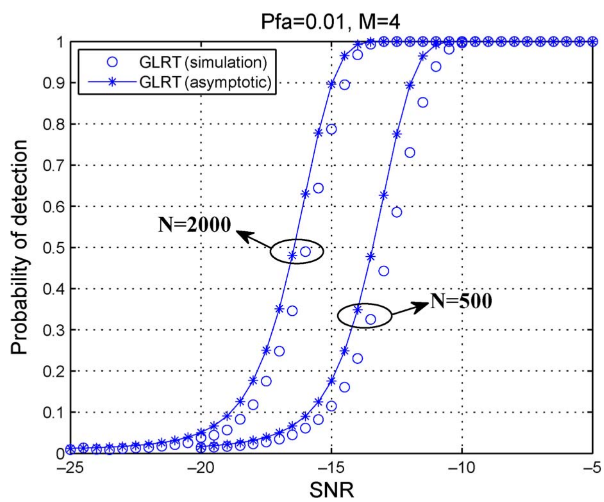

Fig. 6. Comparison between the asymptotic and simulated performance for the proposed GLRT.

of performance improvement from $N = 4$ to $N = 8$ and from $N = 500$ to $N = 2000$ are both about 3 dB, which suggests that the performance of the GLRT improves fast when N is small. Comparison between the asymptotic performance of detection and simulated results is shown in Fig. 6. The results show that the asymptotic results provide close prediction of the detection performance of the GLRT, particularly when the number of samples is large.

VI. Conclusion

A GLRT for spectrum sensing for CR applications has been proposed by exploiting the signal structure to either reduce the number of samples that are required to obtain good performance or improve the performance obtainable from a fixed number of samples. The underlying ML estimates of the GLRT scheme have been developed and expressed in closed forms, supporting the type of real-time implementation that is needed for vehicular applications. The asymptotic performance of the proposed GLRT has also been derived. Simulation results verify that the proposed GLRT produces better performance than the multichannel ED, the AGM detector, and the MME detector, particularly in the case of limited samples, which is a crucial enabler for rapid adaptation that is needed in future vehicular applications. Moreover, closed-form expressions for the detection performance of the multichannel ED have been derived for performance comparison. Our future plan is to develop GLRT spectrum sensing for a general rank-K case, where $1 \leq K \leq M$, and to characterize algorithm performance in dynamic random processes of vehicular applications in urban settings with challenging vehicular-application spectra such as the New York City area, where this research is being conducted.

Appendix I
Maximum-Likelihood Estimates Under H_0 and H_1

A. ML Estimate Under H_0

Under H_0, σ_w^2 is the only unknown parameter. The ML estimate of σ_w^2 can be obtained by taking the derivative of (8) with respect to σ_w^2 and equaling to zero, which is given as

$$\hat{\sigma}^2_{w,H_0} = \frac{1}{M}\sum_{m=1}^{M}\hat{\lambda}_m \tag{23}$$

where we use the fact that $\sum_{m=1}^{M}\hat{\lambda}_m = \text{tr}\{\hat{\mathbf{R}}_x\}$.

B. ML Estimate Under H_1

Under H_1, there are two unknown parameters, i.e., $\mathbf{h}$ and the noise variance σ_w^2. From (9), the log-likelihood function under H_1 is given as

$$\ln p\left(\mathbf{X}\,|\,H_1, \mathbf{h}, \sigma_w^2\right) = -MN\ln(\pi) - N\ln\left|\mathbf{h}\mathbf{h}^H + \sigma_w^2\mathbf{I}\right| - \text{tr}\left\{\mathbf{X}^H\left(\mathbf{h}\mathbf{h}^H + \sigma_w^2\mathbf{I}\right)^{-1}\mathbf{X}\right\}. \tag{24}$$

Maximizing (24) is equivalent to the following minimization:

$$\min_{\mathbf{h},\sigma_w^2} N\,\ln\left|\mathbf{h}\mathbf{h}^H + \sigma_w^2\mathbf{I}\right| + N\,\text{tr}\left\{\frac{1}{N}\mathbf{X}^H\left(\mathbf{h}\mathbf{h}^H + \sigma_w^2\mathbf{I}\right)^{-1}\mathbf{X}\right\}. \tag{25}$$

By expressing $\mathbf{h}$ as a product of a real scalar α and a normalized vector $\bar{\mathbf{h}}$, i.e., $\mathbf{h} = \alpha\bar{\mathbf{h}}$ with $\bar{\mathbf{h}}^H\bar{\mathbf{h}} = 1$, we have

$$\left|\mathbf{h}\mathbf{h}^H + \sigma_w^2\mathbf{I}\right| = \left(\alpha^2 + \sigma_w^2\right)\sigma_w^{2(M-1)} \tag{26}$$

$$\text{tr}\left\{\frac{1}{N}\mathbf{X}^H\left(\mathbf{h}\mathbf{h}^H + \sigma_w^2\mathbf{I}\right)^{-1}\mathbf{X}\right\} \overset{(a)}{=} \frac{\text{tr}(\mathbf{X}^H\mathbf{X})}{N\sigma_w^2} - \frac{\sigma_w^{-4}}{\alpha^{-2} + \sigma_w^{-2}}\frac{1}{N}\text{tr}\{\bar{\mathbf{h}}^H\mathbf{X}\mathbf{X}^H\bar{\mathbf{h}}\} \tag{27}$$

where (a) follows from the Woodbury identity [26]. As a result, the ML estimate of $\bar{\mathbf{h}}$ is the solution of the following constrained optimization:

$$\max_{\bar{\mathbf{h}}} \quad \frac{1}{N}\text{tr}\{\bar{\mathbf{h}}^H\mathbf{X}\mathbf{X}^H\bar{\mathbf{h}}\} \quad \text{s.t.} \quad \bar{\mathbf{h}}^H\bar{\mathbf{h}} = 1 \tag{28}$$

which leads to

$$\bar{\mathbf{h}}_{\text{ML}} = \mathbf{U}_x[:, 1] \tag{29}$$

where $\mathbf{U}_x$ is obtained by carrying out the EVD of the sample covariance matrix, i.e., $\hat{\mathbf{R}}_x = \mathbf{X}\mathbf{X}^H/N = \mathbf{U}_x\mathbf{D}_x\mathbf{U}_x^H$, and the diagonal elements of $\mathbf{D}_x$ are in a descending order. In other words, the ML estimate of $\bar{\mathbf{h}}$ is the eigenvector of the $\hat{\mathbf{R}}_x$ associated with the largest eigenvalue.

Substituting the above $\bar{\mathbf{h}}_{\text{ML}}$ back into (25), the ML estimate of α can be obtained by solving

$$\min_{\alpha} \quad \ln\left(\alpha^2 + \sigma_w^2\right) - \frac{\hat{\lambda}_1}{\sigma_w^2}\frac{\alpha^2}{\alpha^2 + \sigma_w^2}. \tag{30}$$

Let $\beta = \alpha^2 + \sigma_w^2$. Then, (30) is re-expressed as

$$\min_{\beta} \quad \ln\beta - \frac{\hat{\lambda}_1}{\sigma_w^2}\left(1 - \frac{\sigma_w^2}{\beta}\right). \tag{31}$$

The above optimization can be solved by setting its first derivative to be zero, i.e.,

$$\beta = \hat{\lambda}_1 \tag{32}$$

and consequently, α^2 is solved as

$$\alpha_{\text{ML}}^2 = \hat{\lambda}_1 - \sigma_w^2. \tag{33}$$

We now have successfully found the ML estimates of $\{\alpha, \bar{\mathbf{h}}\}$ given a fixed noise variance σ_w^2. It is shown that α_{ML} is dependent on the noise variance σ_w^2, while $\bar{\mathbf{h}}_{\text{ML}}$ is independent of σ_w^2. By substituting the optimum solution $\{\alpha_{\text{ML}}, \bar{\mathbf{h}}_{\text{ML}}\}$ back into (25), the objective function becomes

$$\begin{aligned}
&\frac{N}{2}\ln\left(\sigma_w^{2(M-1)}\left(\alpha_{\text{ML}}^2 + \sigma_w^2\right)\right)\\
&\quad + \frac{1}{2}\text{tr}\left\{\mathbf{X}^H\left(\alpha_{\text{ML}}^2\bar{\mathbf{h}}_{\text{ML}}\bar{\mathbf{h}}_{\text{ML}}^H + \sigma_w^2\mathbf{I}\right)^{-1}\mathbf{X}\right\}\\
&\quad \overset{(a)}{=} \frac{N(M-1)}{2}\ln\sigma_w^2 + \frac{N}{2}\ln\left(\alpha_{\text{ML}}^2 + \sigma_w^2\right)\\
&\qquad + \frac{N\sum_{m=1}^{M}\hat{\lambda}_m}{2\sigma_w^2} - \frac{N\hat{\lambda}_1}{2\sigma_w^2}\frac{\alpha_{\text{ML}}^2}{\alpha_{\text{ML}}^2 + \sigma_w^2}\\
&\quad = \frac{N(M-1)}{2}\ln\sigma_w^2 + \frac{N\sum_{m=1}^{M}\hat{\lambda}_m}{2\sigma_w^2} - \frac{N\hat{\lambda}_1}{2\sigma_w^2}\\
&\qquad + \frac{N}{2}\ln\left(\frac{\hat{\lambda}_1}{N}\right) + \frac{N}{2}
\end{aligned} \tag{34}$$

where (a) comes from (27), and $\bar{\mathbf{h}}_{\text{ML}}^H\mathbf{X}\mathbf{X}^H\bar{\mathbf{h}}_{\text{ML}} = \hat{\lambda}_1$. Therefore, the optimum σ_w^2 can be determined from the following optimization:

$$\min_{\sigma_w^2} \quad \frac{N(M-1)}{2}\ln\sigma_w^2 + \frac{N\sum_{m=1}^{M}\hat{\lambda}_m}{2\sigma_w^2} - \frac{N\hat{\lambda}_1}{2\sigma_w^2} \tag{35}$$

which can be easily solved as

$$\hat{\sigma}_{w,H_1}^2 = \frac{1}{M-1}\sum_{m=2}^{M}\hat{\lambda}_m. \tag{36}$$

Appendix II
Derivation of the GLRT

By substituting the ML estimates, i.e., (23), (29), (33), and (36), under both hypotheses back into (8) and (9) and with the help of (26) and (34), the log-likelihood function can be simplified to

$$\begin{aligned}
&\ln p\left(\mathbf{X} \mid H_0, \hat{\sigma}_{w,H_0}^2\right)\\
&\quad = -\frac{MN}{2}\left[\ln(2\pi) + 1\right] - \frac{MN}{2}\ln\left(\frac{1}{M}\sum_{m=1}^{M}\hat{\lambda}_m\right)
\end{aligned} \tag{37}$$

$$\begin{aligned}
&\ln p\left(\mathbf{X} \mid H_1, \hat{\sigma}_{w,H_1}^2, \hat{\mathbf{h}}_{\text{ML}}\right)\\
&\quad = -\frac{MN}{2}\left[\ln(2\pi) + 1\right] - \frac{N(M-1)}{2}\ln\left(\frac{1}{M-1}\sum_{m=2}^{M}\hat{\lambda}_m\right)\\
&\qquad - \frac{N}{2}\ln(\hat{\lambda}_1).
\end{aligned} \tag{38}$$

Ignoring some constant terms, the log-GLRT statistic is equivalent to

$$\begin{aligned}
T_{\log\text{-GLR}} = MN\ln\left(\frac{1}{M}\sum_{m=1}^{M}\hat{\lambda}_m\right) - N\ln(\hat{\lambda}_1)\\
- (M-1)N\ln\left(\frac{1}{M-1}\sum_{m=2}^{M}\hat{\lambda}_m\right)
\end{aligned} \tag{39}$$

which can be further simplified to

$$T_{\text{GLR}} \propto \frac{1}{\frac{\hat{\lambda}_1}{\sum_{m=1}^{M}\hat{\lambda}_m}\left(1 - \frac{\hat{\lambda}_1}{\sum_{m=1}^{M}\hat{\lambda}_m}\right)^{M-1}}. \tag{40}$$

Note that

$$\frac{1}{M} \le \frac{\hat{\lambda}_1}{\sum_{m=1}^{M}\hat{\lambda}_m} \le 1 \tag{41}$$

and the function $f(x) = 1/x(1-x)^{M-1}$ is monotonically increasing over $x \in (1/M, 1)$. As a result, the GLRT statistic reduces to

$$\text{GLR} = \frac{\hat{\lambda}_1}{\sum_{m=1}^{M}\hat{\lambda}_m}. \tag{42}$$

APPENDIX III
ASYMPTOTIC PERFORMANCE OF THE GLRT

The signal covariance matrix can be rewritten as $\mathbf{R}_s = \xi\bar{\mathbf{h}}\bar{\mathbf{h}}^H$, where ξ is a positive real number, and $\bar{\mathbf{h}}$ is a unit-one complex vector such that $\bar{\mathbf{h}}^H\bar{\mathbf{h}} = 1$. Note that solutions $\bar{\mathbf{h}}$ and $\bar{\mathbf{h}}e^{j\phi}$ yield the same noise-free data, where $e^{j\phi}$ is an additional phase term. As a result, the problem is not identifiable in the sense that the unknown parameters cannot be uniquely determined from noise-free data. To eliminate the "phase ambiguity," we put an additional constraint on the normalized complex vector by assuming

$$\bar{\mathbf{h}} = \begin{bmatrix} \vartheta \\ \bar{\mathbf{h}}_{M-1} \end{bmatrix} \tag{43}$$

where ϑ is a real number that is less than 1. In other words, the first element of the normalized vector $\bar{\mathbf{h}}$ is fixed to a real number.

Following this, the detection problem can be parameterized as

$$\begin{aligned} H_0: \quad & \boldsymbol{\theta}_r = \boldsymbol{\theta}_{r_0}, \boldsymbol{\theta}_s \\ H_1: \quad & \boldsymbol{\theta}_r = \boldsymbol{\theta}_{r_1}, \boldsymbol{\theta}_s \end{aligned} \tag{44}$$

where $\boldsymbol{\theta}_{r_1} = [\xi, \mathrm{vec}\{\mathrm{Re}(\bar{\mathbf{h}}_{M-1})\}, \mathrm{vec}\{\mathrm{Im}(\bar{\mathbf{h}}_{M-1})\}]^T$, $\theta_s = \sigma_w^2$, and $\boldsymbol{\theta}_{r_0} = \mathbf{0}_{2M-1}$. Note that ϑ can be uniquely determined if $\bar{\mathbf{h}}_{M-1}$ is determined due to $\vartheta^2 + \bar{\mathbf{h}}_{M-1}^H\bar{\mathbf{h}}_{M-1} = 1$. In total, there are $2M-1$ unknown signal parameters and one unknown nuisance parameter.

From the above formulation, the asymptotic distribution of the GLRT statistic is [9]

$$T_{\mathrm{GLRT}} \overset{a}{\sim} \begin{cases} \chi^2_{2M-1}, & \text{under } H_0 \\ \chi'^2_{2M-1}(\lambda), & \text{under } H_1 \end{cases} \tag{45}$$

where the noncentrality parameter λ is given by

$$\lambda = (\boldsymbol{\theta}_{r_1} - \boldsymbol{\theta}_{r_0})^T \left(\left[\mathbf{I}^{-1}(\boldsymbol{\theta}_{r_0}, \boldsymbol{\theta}_s) \right]_{\boldsymbol{\theta}_r, \boldsymbol{\theta}_r} \right)^{-1} (\boldsymbol{\theta}_{r_1} - \boldsymbol{\theta}_{r_0}). \tag{46}$$

In the following, the noncentrality parameter λ is derived in closed form.

A. Fisher Information Matrix

The elements of the Fisher information matrix can be calculated as second derivatives of the log-likelihood function with respect to unknown parameters, which are shown as

$$\begin{aligned} -E\left\{\frac{\partial^2 \ln f(\boldsymbol{\theta})}{\partial \varepsilon^2}\right\} = &-\frac{NM}{\varepsilon^2} + \frac{N(2\varepsilon+\xi)\xi}{\varepsilon^2+\varepsilon\xi} \\ &+ \frac{2N(M\varepsilon+\xi)}{\varepsilon^3} + \frac{2N\xi}{\varepsilon^2(\xi+\varepsilon)} \\ &- \frac{2N\xi(\xi+2\varepsilon)}{\varepsilon^2(\xi+\varepsilon)^2} \end{aligned} \tag{47}$$

$$-E\left\{\frac{\partial^2 \ln f(\boldsymbol{\theta})}{\partial \varepsilon \partial \xi}\right\} = \frac{N}{(\varepsilon+\xi)^2} \tag{48}$$

$$-E\left\{\frac{\partial^2 \ln f(\boldsymbol{\theta})}{\partial \xi^2}\right\} = \frac{N}{(\varepsilon+\xi)^2} \tag{49}$$

$$-E\left\{\frac{\partial^2 \ln f(\boldsymbol{\theta})}{\partial \bar{\mathbf{h}}_{R_i} \partial \varepsilon}\right\} = \frac{2N\xi(2\varepsilon+\xi)\bar{\mathbf{h}}_{R_i}}{\varepsilon^2(\varepsilon+\xi)} \tag{50}$$

$$-E\left\{\frac{\partial^2 \ln f(\boldsymbol{\theta})}{\partial \bar{\mathbf{h}}_{I_i} \partial \varepsilon}\right\} = \frac{2N\xi(2\varepsilon+\xi)\bar{\mathbf{h}}_{I_i}}{\varepsilon^2(\varepsilon+\xi)} \tag{51}$$

$$-E\left\{\frac{\partial^2 \ln f(\boldsymbol{\theta})}{\partial \bar{\mathbf{h}}_{R_i} \partial \xi}\right\} = -\frac{2N\bar{\mathbf{h}}_{R_i}}{\varepsilon+\xi} \tag{52}$$

$$-E\left\{\frac{\partial^2 \ln f(\boldsymbol{\theta})}{\partial \bar{\mathbf{h}}_{I_i} \partial \xi}\right\} = -\frac{2N\bar{\mathbf{h}}_{I_i}}{\varepsilon+\xi} \tag{53}$$

$$-E\left\{\frac{\partial^2 \ln f(\boldsymbol{\theta})}{\partial \bar{\mathbf{h}}_{R_i} \partial \bar{\mathbf{h}}_{R_l}}\right\} = \begin{cases} -\frac{2N\xi\left(\bar{\mathbf{h}}_{R_i}\bar{\mathbf{h}}_{R_l} + \bar{\mathbf{h}}_{I_i}\bar{\mathbf{h}}_{I_l}\right)}{\varepsilon(\varepsilon+\xi)}, & \text{if } i \neq l \\ -\frac{2N\xi\left(\bar{\mathbf{h}}^2_{R_i} + \bar{\mathbf{h}}^2_{I_i} + \sigma_w^2\right)}{\varepsilon(\varepsilon+\xi)}, & \text{if } i = l \end{cases} \tag{54}$$

$$-E\left\{\frac{\partial^2 \ln f(\boldsymbol{\theta})}{\partial \bar{\mathbf{h}}_{R_i} \partial \bar{\mathbf{h}}_{I_l}}\right\} = \begin{cases} \frac{2N\xi\left(\bar{\mathbf{h}}_{I_i}\bar{\mathbf{h}}_{R_l} - \bar{\mathbf{h}}_{R_i}\bar{\mathbf{h}}_{I_l}\right)}{\varepsilon(\varepsilon+\xi)}, & \text{if } i \neq l \\ 0, & \text{if } i = l \end{cases} \tag{55}$$

$$-E\left\{\frac{\partial^2 \ln f(\boldsymbol{\theta})}{\partial \bar{\mathbf{h}}_{I_i} \partial \bar{\mathbf{h}}_{I_l}}\right\} = \begin{cases} -\frac{2N\xi\left(\bar{\mathbf{h}}_{R_i}\bar{\mathbf{h}}_{R_l} + \bar{\mathbf{h}}_{I_i}\bar{\mathbf{h}}_{I_l}\right)}{\varepsilon(\varepsilon+\xi)}, & \text{if } i \neq l \\ -\frac{2N\xi\left(\bar{\mathbf{h}}^2_{R_i} + \bar{\mathbf{h}}^2_{I_i} + \sigma_w^2\right)}{\varepsilon(\varepsilon+\xi)}, & \text{if } i = l \end{cases} \tag{56}$$

$$-E\left\{\frac{\partial^2 \ln f(\boldsymbol{\theta})}{\partial \bar{\mathbf{h}}_{I_i} \partial \bar{\mathbf{h}}_{R_l}}\right\} = \begin{cases} -\frac{2N\xi\left(\bar{\mathbf{h}}_{I_i}\bar{\mathbf{h}}_{R_l} - \bar{\mathbf{h}}_{R_i}\bar{\mathbf{h}}_{I_l}\right)}{\varepsilon(\varepsilon+\xi)}, & \text{if } i \neq l \\ 0, & \text{if } i = l \end{cases} \tag{57}$$

where $\varepsilon = \sigma_w^2$ for notation simplicity.

B. Noncentrality Parameter

By evaluating the above Fisher information at $\boldsymbol{\theta}_r = \boldsymbol{\theta}_{r_0} = \mathbf{0}_{2M-1}$ and $\theta_s = \theta_s$, we have

$$\begin{aligned} &\mathbf{I}_{\boldsymbol{\theta}_r,\boldsymbol{\theta}_r}(\boldsymbol{\theta}_{r_0}, \theta_s) \\ &= \begin{bmatrix} \frac{N}{\varepsilon^2} & \mathbf{0}_{1\times(M-1)} & \mathbf{0}_{1\times(M-1)} \\ \mathbf{0}_{(M-1)\times 1} & \mathbf{0}_{(M-1)\times(M-1)} & \mathbf{0}_{(M-1)\times(M-1)} \\ \mathbf{0}_{(M-1)\times 1} & \mathbf{0}_{(M-1)\times(M-1)} & \mathbf{0}_{(M-1)\times(M-1)} \end{bmatrix} \end{aligned}$$

$$\mathbf{I}_{\boldsymbol{\theta}_r,\theta_s}(\boldsymbol{\theta}_{r_0}, \theta_s) = \begin{bmatrix} \frac{N}{\varepsilon^2} \\ \mathbf{0}_{(M-1)\times 1} \\ \mathbf{0}_{(M-1)\times 1} \end{bmatrix} \quad \mathbf{I}_{\theta_s,\theta_s} = \frac{NM}{\varepsilon^2}.$$

With $\boldsymbol{\theta}_{r_1} = [\xi, \mathrm{vec}\{\mathrm{Re}(\bar{\mathbf{h}}_{M-1})\}, \mathrm{vec}\{\mathrm{Im}(\bar{\mathbf{h}}_{M-1})\}]^T$ and $\boldsymbol{\theta}_{r_0} = \mathbf{0}_{2M-1}$, the noncentrality parameter λ can be determined as

$$\begin{aligned} \lambda &= (\boldsymbol{\theta}_{r_1} - \boldsymbol{\theta}_{r_0})^T \left(\left[\mathbf{I}^{-1}(\boldsymbol{\theta}_{r_0}, \boldsymbol{\theta}_s) \right]_{\boldsymbol{\theta}_r, \boldsymbol{\theta}_r} \right)^{-1} (\boldsymbol{\theta}_{r_1} - \boldsymbol{\theta}_{r_0}) \\ &= \frac{N(M-1)\xi^2}{M\varepsilon^2} = \frac{N(M-1)(\mathbf{h}^H\mathbf{h})^2}{M\left(\sigma_w^2\right)^2}. \end{aligned} \tag{58}$$

APPENDIX IV
PERFORMANCE OF THE MULTICHANNEL ED

A. Exact Performance of the Multichannel ED

For easy references, we repeat the test statistic of the multichannel ED, i.e.,

$$V = \sum_{n=0}^{N-1} \|(n)\|^2 . \tag{59}$$

Under H_0, V is the sum of the square of $2MN$ independent and identical Gaussian random variables with zero mean and variance $\sigma_w^2/2$, while V, under H_1, sums the square of $2MN$ independent Gaussian random variables conditioned on $\mathbf{h}$. As such, the distribution of the test statistic can be expressed as

$$H_0: \quad V \sim \frac{\sigma_w^2}{2}\chi_{2MN}^2 \tag{60}$$

$$H_1: \quad V \sim \frac{\sigma_w^2}{2}\chi_{2MN}^{\prime 2}(2\rho) \tag{61}$$

where the noncentrality parameter $2\rho = 2N\mathrm{tr}\{\mathbf{R}_s\}/\sigma_w^2$. Based on the above distributions, the probabilities of false alarm and detection can be calculated as

$$\begin{aligned} P_f &= \int_\gamma^\infty f(V \mid H_0)\, dV \\ &= \frac{2}{\sigma_w^2}\int_\gamma^\infty \frac{1}{2^{MN}\Gamma(MN)}\left(\frac{2x}{\sigma_w^2}\right)^{MN-1} \exp\left\{-\frac{x}{\sigma_w^2}\right\} dx \\ &= \frac{\bar{\Gamma}\left(MN, \gamma/\sigma_w^2\right)}{\Gamma(MN)} \end{aligned} \tag{62}$$

$$\begin{aligned} P_d &= \int_\gamma^\infty f(V \mid H_1)\, dV \\ &= \frac{2}{\sigma_w^2}\int_\gamma^\infty \frac{1}{2} e^{-\frac{x+\rho\sigma_w^2}{\sigma_w^2}} \left(\frac{x}{\rho\sigma_w^2}\right)^{\frac{MN-1}{2}} I_{(MN-1)}\left(\sqrt{\frac{4\rho x}{\sigma_w^2}}\right) dx \\ &= Q_{MN}\left(\sqrt{2\rho}, \sqrt{\frac{2\gamma}{\sigma_w^2}}\right). \end{aligned} \tag{63}$$

Under the condition that the noise variance is unknown, the multichannel ED (3) has to estimate the noise variance as $\hat{\sigma_w^2} = \eta\sigma_w^2$. In this case, the threshold is selected by using the estimated noise variance $\hat{\sigma_w^2}$, and, therefore, the probabilities of false alarm and detection can be similarly calculated as

$$P_f = \frac{\bar{\Gamma}\left(MN, \gamma/\left(\eta\sigma_w^2\right)\right)}{\Gamma(MN)} \tag{64}$$

$$P_d = Q_{MN}\left(\sqrt{2\rho}, \sqrt{\frac{2\gamma}{\sigma_w^2}}\right). \tag{65}$$

B. Asymptotic Performance of the Multichannel ED

When the number of samples is large, the test statistic can be approximated as a Gaussian random variable under either of the hypotheses according to the central limit theorem, i.e.,

$$H_0: \quad V \sim \mathcal{N}\left(MN\sigma_w^2, MN\sigma_w^4\right) \tag{66}$$

$$H_1: \quad V \sim \mathcal{N}\left(MN\sigma_w^2 + NP_s, MN\sigma_w^4 + 2N\sigma_w^2 P_s\right) \tag{67}$$

where P_s represents the primary signal power over M receive antennas. Thus, the asymptotic P_f and P_d for the multichannel ED (2) are

$$P_f = Q\left(\frac{\gamma - MN\eta\sigma_w^2}{\sigma_w^2\sqrt{MN}}\right) \tag{68}$$

$$P_d = Q\left(\frac{\gamma - MN\eta\sigma_w^2 - NP_s}{\sigma_w\sqrt{MN\sigma_w^2 + 2NP_s}}\right) \tag{69}$$

while the counterparts for the multichannel ED with noise uncertainty (3) are

$$P_f = Q\left(\frac{\gamma - MN\eta\sigma_w^2}{\eta\sigma_w^2\sqrt{MN}}\right) \tag{70}$$

$$P_d = Q\left(\frac{\gamma - MN\sigma_w^2 - NP_s}{\sigma_w\sqrt{MN\sigma_w^2 + 2NP_s}}\right) \tag{71}$$

where

$$Q(x) = \frac{1}{\sqrt{2\pi}}\int_x^\infty e^{-\tau^{2/2}}\, d\tau. \tag{72}$$

ACKNOWLEDGMENT

The authors would like to thank Dr. J. Mitola, III, for his helpful comments and suggestions on this paper.

REFERENCES

[1] Fed. Commun. Comm., *Spectrum Policy Task Force*. [Online]. Available: http://www.fcc.gov/sptf/
[2] J. Mitola, III, "Cognitive radio," Licentiate thesis, Roy. Inst. Technol., Stockholm, Sweden, 1999.
[3] J. Mitola, III, "Cognitive radio for flexible mobile multimedia communications," in *Proc. IEEE Mobile Multimedia Commun. Conf.*, San Diego, CA, Nov. 1999, pp. 3–10.
[4] S. Haykin, "Cognitive radio: Brain-empowered wireless communications," *IEEE J. Sel. Areas Commun.*, vol. 23, no. 2, pp. 201–220, Feb. 2005.
[5] J. Ma, G. Y. Li, and B. H. Juang, "Signal processing in cognitive radio," *Proc. IEEE*, vol. 97, no. 5, pp. 805–823, May 2009.
[6] R. Tandra, S. M. Mishra, and A. Sahai, "What is a spectrum hole and what does it take to recognize one?" in *Proc. IEEE*, vol. 97, no. 5, pp. 824–848, May 2009.
[7] S. Haykin, D. J. Thomson, and J. H. Reed, "Spectrum sensing for cognitive radio," *Proc. IEEE*, vol. 97, no. 5, pp. 849–877, May 2009.
[8] A. Sahai and D. Cabric, "Spectrum sensing: Fundamental limits and practical challenges," in *Proc. IEEE Int. Symp. New Frontiers DySPAN (Tutorial)*, Baltimore, MD, Nov. 2005. [Online]. Available: http://www.eecs.berkeley.edu/~sahai/Presentations/Dyspan_2005_tutorial_part_I.pdf
[9] S. M. Kay, *Fundamentals of Statistical Signal Processing: Detection Theory*. Upper Saddle River, NJ: Prentice-Hall, 1998.

[10] H. S. Chen, W. Gao, and D. G. Daut, "Signature based spectrum sensing algorithms for IEEE 802.22 WRAN," in *Proc. IEEE Int. Conf. Commun.*, Glasgow, U.K., Jun. 24–28, 2007, pp. 6487–6492.

[11] D. Cabric, A. Tkachenko, and R. W. Brodersen, "Spectrum sensing measurements of pilot, energy, and collaborative detection," in *Proc. MILCOM*, Washington, DC, Oct. 23–25, 2006, pp. 1–7.

[12] H. Urkowitz, "Energy detection of unknown deterministic signals," *Proc. IEEE*, vol. 55, no. 4, pp. 523–531, Apr. 1967.

[13] A. Sonnenschein and P. M. Fishman, "Radiometric detection of spread-spectrum signals in noise of uncertain power," *IEEE Trans. Aerosp. Electron. Syst.*, vol. 28, no. 3, pp. 654–660, Jul. 1992.

[14] V. I. Kostylev, "Energy detection of a signal with random amplitude," in *Proc. IEEE ICC*, Apr. 2002, vol. 3, pp. 1606–1610.

[15] F. F. Digham, M. S. Alouini, and M. K. Simon, "On the energy detection of unknown signals over fading channels," *IEEE Trans. Commun.*, vol. 55, no. 1, pp. 21–24, Jan. 2007.

[16] W. A. Gardner, "Signal interception: A unifying theoretical framework for feature detection," *IEEE Trans. Commun.*, vol. 36, no. 8, pp. 897–906, Aug. 1988.

[17] W. Gardner, "A new method of channel identification," *IEEE Trans. Commun.*, vol. 39, no. 6, pp. 813–817, Jun. 1991.

[18] P. D. Sutton, K. E. Nolan, and L. E. Doyle, "Cyclostationary signatures in practical cognitive radio applications," *IEEE J. Sel. Areas Commun.*, vol. 26, no. 1, pp. 13–24, Jan. 2008.

[19] D. Cabric, S. M. Mishra, and R. W. Brodersen, "Implementation issues in spectrum sensing for cognitive radios," in *Proc. 38th Asilomar Conf. Syst. Comput.*, Pacific Grove, CA, Nov. 7–11, 2004, pp. 772–776.

[20] R. Tandra and A. Sahai, "Fundamental limits on detection in low SNR under noise uncertainty," in *Proc. Int. Conf. Wireless Netw., Commun. Mobile Comput.*, Maui, HI, Jun. 13–16, 2005, pp. 464–469.

[21] Y. Zeng and Y. C. Liang, "Maximum–minimum eigenvalue detection for cognitive radio," in *Proc. IEEE 18th Int. Symp. Pers., Indoor, Mobile Radio Commun.*, Athens, Greece, Sep. 3–7, 2007, pp. 1–5.

[22] T. J. Lim, R. Zhang, Y. C. Liang, and Y. Zeng, "GLRT-based spectrum sensing for cognitive radio," in *Proc. IEEE Global Telecommun. Conf.*, New Orleans, LA, Nov. 30–Dec. 4, 2008, pp. 1–5.

[23] S. M. Kay, *Fundamentals of Statistical Signal Processing: Estimation Theory*. Upper Saddle River, NJ: Prentice-Hall, 1993.

[24] H. Li, X. Lu, and G. B. Giannakis, "Capon multiuser receiver for CDMA systems with space–time coding," *IEEE Trans. Signal Process.*, vol. 50, no. 5, pp. 1193–1204, May 2002.

[25] M. Abramowitz and I. A. Ryzhik, *Handbook of Mathematical Functions With Formulas, Graphs, and Mathematical Tables*. New York: Dover, 1972.

[26] R. A. Horn and C. R. Johnson, *Matrix Analysis*. Cambridge, U.K.: Cambridge Univ. Press, 1985.

Pu Wang (S'05) received the B.Eng. and M.Eng. degrees in electrical engineering from the University of Electronic Science and Technology of China, (UESTC), Chengdu, China, in 2003 and 2006, respectively. He is currently working toward the Ph.D. degree with the Department of Electrical and Computer Engineering, Stevens Institute of Technology, Hoboken, NJ.

From January 2007 to December 2007, he was a Research Assistant and, from January 2008 to December 2008, he was a Teaching Assistant with the Department of Electrical and Computer Engineering, Stevens Institute of Technology, where he is currently a Research Assistant. His current research interests include statistical signal processing and its applications, with focus on detection and estimation, multichannel signal processing, and nonstationary signal processing.

Mr. Wang was a recipient of the Francis T. Boesch Award in 2008 and the Outstanding Research Assistant Award in 2007 from Stevens Institute of Technology, the Excellent Master Thesis Award of Sichuan Province in 2007, and the Excellent Master Thesis Award from UESTC in 2006.

Jun Fang (M'08) received the B.Sc. and M.Sc. degrees in electrical engineering from Xidian University, Xi'an, China, in 1998 and 2001, respectively, and the Ph.D. degree in electrical engineering from the National University of Singapore, Singapore, in 2006.

In 2006, he was a Postdoctoral Research Associate with the Department of Electrical and Computer Engineering, Duke University, Durham, NC. He is currently a Postdoctoral Research Associate with the Department of Electrical and Computer Engineering, Stevens Institute of Technology, Hoboken, NJ. His research interests include statistical signal processing, wireless communications, and distributed estimation and detection, with their applications to wireless sensor networks.

Ning Han (S'07) received the B.E. degree in electronics engineering from Beijing University of Technology, Beijing, China, in 2004 and the M.E. degree in electrical engineering from Inha University, Incheon, Korea, in 2006. He is currently working toward the Ph.D. degree with the Department of Electrical and Computer Engineering, Stevens Institute of Technology, Hoboken, NJ.

From 2006 to 2009, he was a Research Assistant with the Graduate School of Information Technology and Telecommunications, Inha University. He is currently a Research Assistant with the Department of Electrical and Computer Engineering, Stevens Institute of Technology. His current research interests include statistical signal processing, wireless communications, and signal detection and estimation, with their applications to cognitive radios.

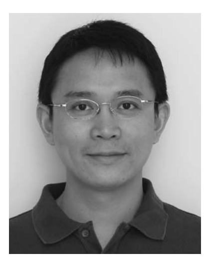

Hongbin Li (M'99–SM'09) received the B.S. and M.S. degrees in electrical engineering from the University of Electronic Science and Technology of China, Chengdu, China, in 1991 and 1994, respectively, and the Ph.D. degree in electrical engineering from the University of Florida, Gainesville, in 1999.

From July 1996 to May 1999, he was a Research Assistant with the Department of Electrical and Computer Engineering, University of Florida. Since July 1999, he has been with the Department of Electrical and Computer Engineering, Stevens Institute of Technology, Hoboken, NJ, where he is currently an Associate Professor. In the summers of 2003, 2004, and 2009, he was a Summer Visiting Faculty with the Air Force Research Laboratory, Wright-Patterson Air Force Base, OH. His current research interests include statistical signal processing, wireless communications, and radar.

Dr. Li is a member of Tau Beta Pi and Phi Kappa Phi. He was a recipient of the Harvey N. Davis Teaching Award in 2003 and the Jess H. Davis Memorial Award for excellence in research in 2001 from Stevens Institute of Technology and the Sigma Xi Graduate Research Award from the University of Florida in 1999. He is a Member of the Sensor Array and Multichannel Technical Committee of the IEEE Signal Processing Society. He has been an Editor or an Associate Editor for the IEEE TRANSACTIONS ON WIRELESS COMMUNICATIONS, the IEEE SIGNAL PROCESSING LETTERS, and the IEEE TRANSACTIONS ON SIGNAL PROCESSING and served as a Guest Editor for the *EURASIP Journal on Applied Signal Processing Special Issue on Distributed Signal Processing Techniques for Wireless Sensor Networks*.